Wind and Structures, *Vol. 25, No. 5 (2017) 459-474*
DOI: https://doi.org/10.12989/was.2017.25.5.459

Analytical solution for natural frequency of monopile supported wind turbine towers

Xue-Ning Rong[1], Ri-Qing Xu[*2], Heng-Yu Wang[3] and Su-Yang Feng[2]

[1]*School of Mechanical Engineering, Nanjing University of Science and Technology, Nanjing 210094, China*
[2]*Research center of coastal and urban geotechnical engineering, Zhejiang University, Hangzhou 310058, China*
[3]*Ningbo institute of technology, Zhejiang University, Ningbo 315100, China*

(Received May 25, 2017, Revised August 9, 2017, Accepted August 12, 2017)

Abstract. In this study an analytical expression is derived for the natural frequency of the wind turbine towers supported on flexible foundation. The derivation is based on a Euler-Bernoulli beam model where the foundation is represented by a stiffness matrix. Previously the natural frequency of such a model is obtained from numerical or empirical method. The new expression is based on pure physical parameters and thus can be used for a quick assessment of the natural frequencies of both the real turbines and the small-scale models. Furthermore, a relationship between the diagonal and non-diagonal element in the stiffness matrix is introduced, so that the foundation stiffness can be obtained from either the *p*-*y* analysis or the loading test. The results of the proposed expression are compared with the measured frequencies of six real or model turbines reported in the literature. The comparison shows that the proposed analytical expression predicts the natural frequency with reasonable accuracy. For two of the model turbines, some errors were observed which might be attributed to the difference between the dynamic and static modulus of saturated soils. The proposed analytical solution is quite simple to use, and it is shown to be more reasonable than the analytical and the empirical formulas available in the literature.

Keywords: natural frequency; wind turbine tower; soil-structure interaction; beam theory; stiffness matrix

1. Introduction

The wind turbine towers are dynamically sensitive structures (Bhattacharya *et al.* 2013a, b, Lombardi *et al.* 2013). In order to avoid resonance, the natural frequency of the turbine-foundation system should be kept sufficiently separated from the forcing frequencies due to wind turbulence, waves, the rotational frequency (1P) and the blade passing frequency (2P or 3P). Therefore, the estimation of the natural frequency of the whole system is essential in design calculation (DNV, 2014). However, determining the natural frequency is one of the most challenging tasks. Deviations from the design natural frequencies are observed for some real wind turbine towers (Arany *et al.* 2015, Zaaijer 2006). Since the turbines installed are becoming higher and heavier, the prediction of natural frequency is even more important because the intervals of target frequency are much narrower for heavier turbines (Arany *et al.* 2016).

∗Corresponding author, Professor, E-mail: xurq@zju.edu.cn

http://www.techno-press.org/?journal=was&subpage=8 ISSN: 1226-6116 (Print), 1598-6225 (Online)

In early studies, the wind turbine towers were assumed to be settled on infinitely stiff foundations. The natural frequencies of the fixed-base model can be obtained by analytical or numerical method (Jafri *et al.* 2011, Tempel and Molenaar 2003). However, subsequent works of Zaaijer (2002a, b, 2006) and Bhattacharya *et al.* (2011, 2013a, b) reveal that the foundation stiffness plays an important role in the calculation of natural frequencies. As a result, foundation models are introduced into the dynamic analysis. One of the commonly used model of the foundation is a stiffness matrix, which is also known as three-spring model (Arany *et al.* 2015). Frequency results based on the stiffness matrix are shown to be reasonable predictions for wind turbine towers supported by monopile (Zaaijer 2006). However, the coupled stiffness in the matrix is often ignored (i.e. the uncoupled springs assumption) to obtain an analytical solution. Based on the model of uncoupled springs, analytical expressions have been developed by Adhikari and Bhattacharya (2011, 2012) to calculate the first natural frequency. From a physical point of view, the lateral displacement of the monopile of a wind turbine is mainly induced by the moment, but not the lateral force, thus the coupled stiffness cannot be ignored. A mathematical model (Arany *et al.* 2015) has been provided for the stiffness matrix, but the model leads to a transcendental equation and thus can only be solved numerically. Based on the numerical results of the transcendental equation, Arany *et al.* (2016) proposed an empirical formula for the stiffness matrix. However a clear expression with pure physical parameters is not reported in the literature. Although the numerical method can be used to model the turbine towers with more complicated details, an analytical expression considering a reasonable foundation is still useful to check the numerous combinations of design parameters as a first step. This analytical expression can also provide a physical understanding of natural frequency of a turbine tower. This can be helpful to verify the output from a numerical program, as well as the results of a scale-model test.

The aim of this work is to provide a physical derivation of the first natural frequency based on Rayleigh's method. A new expression based on pure physical parameters is derived for the natural frequency of the turbine towers, for which the foundation is modelled as a stiffness matrix. The expression is then validated against the experimental measurements for both the real turbines and the small-scale models. Furthermore, a relationship is introduced between the diagonal and non-diagonal element in the stiffness matrix, such that the foundation stiffness can be obtained from either the commonly used *p-y* analysis or the static loading test. A comparison is also made between the new expression and other formulas available in the literature.

2. Models of wind turbine-foundation system

Dimensions of a typical wind turbine tower and the mathematical models are shown in Fig. 1. The pile above the mudline is not considered in the upper structure because (i) for a real wind turbine tower, the bending stiffness of the monopile is far more larger than that of the tower, and (ii) an early study (Zaaijer 2006) shows that the kinetic energy of the monopile is only about four orders of magnitude less than that of the tower, which means the inertia of the pile is negligible. On the other hand, the pile both above and below mudline is considered in the foundation models. Thus the decrease in stiffness (and natural frequency) of the whole system due to deeper water sites is taken into account.

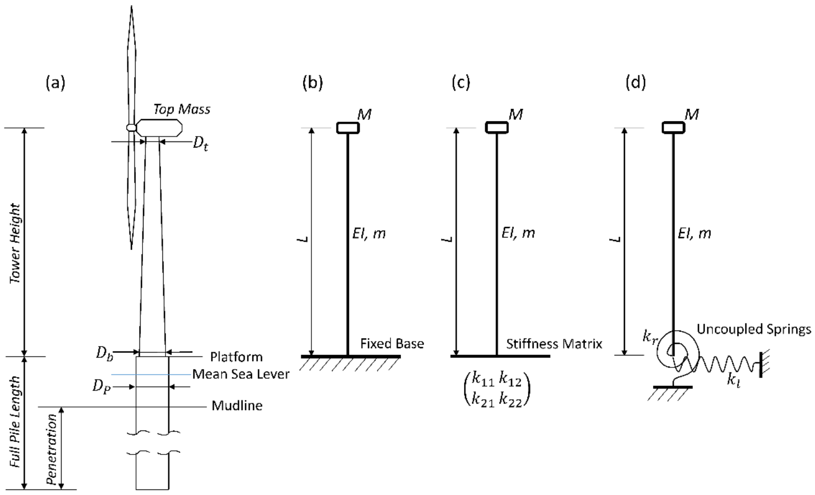

Fig. 1 Dimensions of a wind turbine tower supported by monopile and the mathematical models for dynamic analysis

2.1 Fixed base model of wind turbine tower

Classically, a wind turbine tower is modeled as a cantilever beam with a top mass, *M*. The beam is fixed at the bottom as shown in Fig. 1(b), thus the foundation characteristics are ignored. First natural frequency of that model is given by Blevins (2001)

$$f_{FB} = \frac{1}{2\pi}\sqrt{\frac{3EI}{\left(M + \frac{33}{140}mL\right)L^3}} \tag{1}$$

where L = beam length; EI = bending stiffness of the beam; and m = mass per unit length of the beam. A similar expression for the fixed base model can also be found in Tempel and Molenaar (2003).

The turbine tower is typically a tapered column, thus EI in Eq. (1) should be replaced by an equivalent bending stiffness, EI_{eq}. According to a physical derivation (Arany *et al.* 2016), the equivalent EI is obtained as

$$EI_{eq} = EI_t \times \frac{1}{3} \times \frac{2q^2(q-1)^3}{2q^2 \ln q - 3q^2 + 4q - 1} \qquad \text{with} \quad q = \frac{D_b}{D_t} \tag{2}$$

where EI_t is the bending stiffness at the top of the tower, D_b and D_t denotes the diameter at the bottom and at the top of the tower. For a tower of constant diameter, it can be verified that

$$\lim_{q\to 1}\left[\frac{1}{3} \times \frac{2q^2(q-1)^3}{2q^2 \ln q - 3q^2 + 4q - 1}\right] = 1 \tag{3}$$

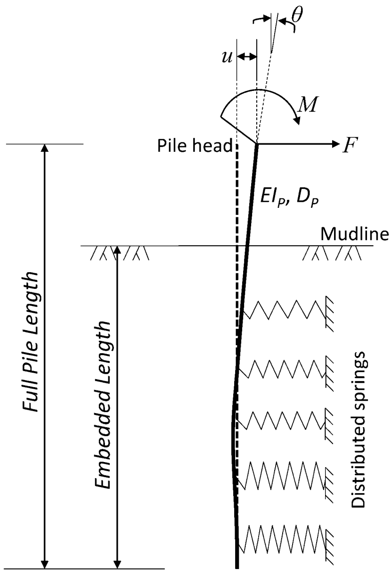

Fig. 2 Foundation model of a laterally loaded pile

Equivalent m of a tapered tower can also be calculated via integration. The final expression is

$$m = \frac{\rho_T V_T}{L} = \frac{\pi}{2}\rho_T t_T\left(D_b + D_t - 2t_T\right) \tag{4}$$

where V_T = volume of the tapered tower; t_T = wall thickness; and ρ_T = density of the tower material. With the equivalent EI and m, the tapered tower is transformed into a uniform beam, thus can be analysed as Figs. 1(b)-1(d).

2.2 Foundation models

A typical model of laterally loaded pile is shown in Fig. 2. D_P, EI_P are the diameter and bending stiffness of the monopile, respectively. If the inertia of the pile is negligible, the behaviour of the foundation can be represented completely by a stiffness matrix (**K**) which describes the relationship between the general load (**F**) and the displacement vector (**u**) at the pile head (Zaaijer 2006).

$$\mathbf{F} = \mathbf{K}\mathbf{u} \qquad \begin{pmatrix} F \\ M \end{pmatrix} = \begin{pmatrix} k_{11} & k_{12} \\ k_{21} & k_{22} \end{pmatrix}\begin{pmatrix} u \\ \theta \end{pmatrix} \tag{5}$$

where F = lateral force; M = moment; u = lateral displacement; θ = dimensionless rotation (in rad); k_{11} = lateral stiffness; k_{22} = rotational stiffness; and k_{12} = k_{21} = coupled stiffness. A more general stiffness matrix will include the element of k_{33}, which describes the vertical stiffness. But during the lateral vibration, the strain energy caused by the vertical displacement is a constant. Thus k_{33} is not relevant in the dynamic analysis.

In order to simplify the model, the non-diagonal element in Eq. (5) is often ignored and the stiffness matrix reduces to uncoupled springs

$$\begin{pmatrix} F \\ M \end{pmatrix} = \begin{pmatrix} k_l & 0 \\ 0 & k_r \end{pmatrix} \begin{pmatrix} u \\ \theta \end{pmatrix} \tag{6}$$

where k_l and k_r denotes the stiffness of the lateral and rotational springs, respectively. In real foundations, the two springs tend to weaken each other during deformation. This can be described by the negative value of k_{12}. Therefore, the foundation stiffness is overestimated in the model of uncoupled springs.

2.3 Empirical method for stiffness matrix

Since the uncoupled springs model might overestimate the first natural frequency, an empirical method is developed by Arany *et al.* (2016) for the model of stiffness matrix. According to the numerical results of a transcendental equation (Arany *et al.* 2015), a closed form expression is fitted as

$$f_1 = C_R C_L f_{FB} \tag{7}$$

where C_R and C_L are dimensionless coefficients. The two coefficients can be expressed as functions of the stiffness parameters

$$C_R = C_R\left(EI, L, k_{11}, k_{22}, k_{12}, a\right) \qquad C_L = C_L\left(EI, L, k_{11}, k_{22}, k_{12}, b\right) \tag{8}$$

in which a and b are empirical constants. Eq. (7) implies that the first natural frequency (f_1) is obtained by multiplying the fixed base frequency by two factors which account for the foundation flexibility. If the pile head is significantly higher than the mudline, another coefficient should be multiplied in Eq. (7). Detailed expressions for this empirical method can be found in Arany *et al.* (2016).

3. Elements in the stiffness matrix

Several methods can be used to determine the stiffness of the foundation. For monopiles embedded in a certain type of soil, some formula methods have been summarized by Zaaijer (2006) and Arany *et al.* (2016). But the real turbine towers are usually founded on complex layered soils, which make it difficult to determine the parameters used in the formulas. Another method to obtain the foundation stiffness is the *p*-*y* analysis recommended by API (2007). The *p*-*y* method is widely used to model the lateral springs as shown in Fig. 2. For each of the soil types, API (2007) presents clear values of the spring parameters, which can also be used for the layered soils. Alternatively, the foundation stiffness can be measured directly from the static loading tests. To avoid the difficulty in choosing parameters, formula methods are not adopted in this study. The stiffness of the foundation is obtained from the *p*-*y* curves or the static loading tests. Although the *p*-*y* curves describe a nonlinear soil behaviour, the monopile foundation of a real wind turbine is generally working in the linear regime (Arany *et al.* 2016). Therefore, the initial stiffness of the foundation is used in this study.

3.1 Cyclic p-y curves

For dynamic analysis, cyclic *p-y* curves are used to represent the lateral soil springs. The *p-y* curves are determined by the soil type and generally based on such parameters: (i) undrained shear strength (s_u) for clays, (ii) effective friction angle (φ') for dry or saturated sands, (iii) dry unit weight (γ_d) or submerged unit weight (γ') of the soil. Detailed formulas for the soil springs can be found in API (2007). Monopile above the mudline is considered as an extra cantilever beam as shown in Fig. 2. With a given load (**F**), displacement vector (**u**) at the pile head is calculated through a FEM method.

From *p-y* analysis, two displacement vectors, $\mathbf{u}_1=(u_1, \theta_1)^T$ and $\mathbf{u}_2=(u_2, \theta_2)^T$, can be calculated for two load cases, $\mathbf{F}_1=(F_1, M_1)^T$ and $\mathbf{F}_2=(F_2, M_2)^T$. To obtain the stiffness matrix, $\mathbf{F}_1$ and $\mathbf{F}_2$ should be linear independent. Then the three elements in the stiffness matrix are given by

$$\begin{pmatrix} k_{11} \\ k_{12} \\ k_{22} \end{pmatrix} = \begin{pmatrix} u_1 & \theta_1 & 0 \\ 0 & u_1 & \theta_1 \\ u_2 & \theta_2 & 0 \end{pmatrix}^{-1} \begin{pmatrix} F_1 \\ M_1 \\ F_2 \end{pmatrix} \tag{9}$$

If $\mathbf{u}_1$ and $\mathbf{u}_2$ are in the linear regime, the obtained stiffness matrix will be independent of the magnitudes of $\mathbf{F}_1$ and $\mathbf{F}_2$.

For the uncoupled springs model, the spring stiffness is usually represented by the initial tangent of the load-displacement curve for each degree of freedom. To obtain an *F-u* curve, the moment *M* is fixed to zero. Substituting *M*=0 into Eq. (5), the stiffness of lateral spring is given by

$$k_l = k_{11} - \frac{k_{12}^{\ 2}}{k_{22}} \tag{10}$$

Similarly, the stiffness of rotational spring is obtained by substituting *F*=0 into Eq. (5).

$$k_r = k_{22} - \frac{k_{12}^{\ 2}}{k_{11}} \tag{11}$$

3.2 Static loading test

Fig. 3 shows two types of static load tests on a monopile (Bhattacharya and Adhikari 2011; Bhattacharya *et al*. 2013b). According to the test results, the spring stiffness (k_l and k_r) are measured directly from the initial tangent of the *F-u* and *M-θ* curve. In order to obtain the three elements in the stiffness matrix, some relationship should be introduced between the diagonal and non-diagonal elements. Based on the *p-y* analysis on a number of monopile foundations, the following relationship is introduced

$$k_{12} = -\delta\sqrt{k_{11}k_{22}} \tag{12}$$

where δ is a dimensionless constant. Elements in the stiffness matrix are calculated for varied monopiles from *p-y* method. The parameters of monopiles are based on real situations with varied pile diameters (0.02-4 m), pile lengths (0.45-30 m) and soil conditions (clayey or sandy layers). Fig. 4 shows the results of calculations as a scatter plot. A linear relationship can be found between

k_{12} and the square root of $k_{11}k_{22}$. Indicated on Fig. 4 are also the approximate ranges of pile diameter (the exact pile diameter depends on other properties of the pile and the soil). It is clear that Eq. (12) captures the relationship between the diagonal and non-diagonal elements with good accuracy, no matter for model piles with very small diameter, or real monopiles of offshore wind turbines. The fitted value of δ is 0.826 with R-square=0.998. According to the formula methods presented by Zaaijer (2006), the value of δ is 0.768 (Randolph's formula) or 0.866 (formula based on the effective fixity length), which is quite close to the value fitted from *p*-*y* analysis.

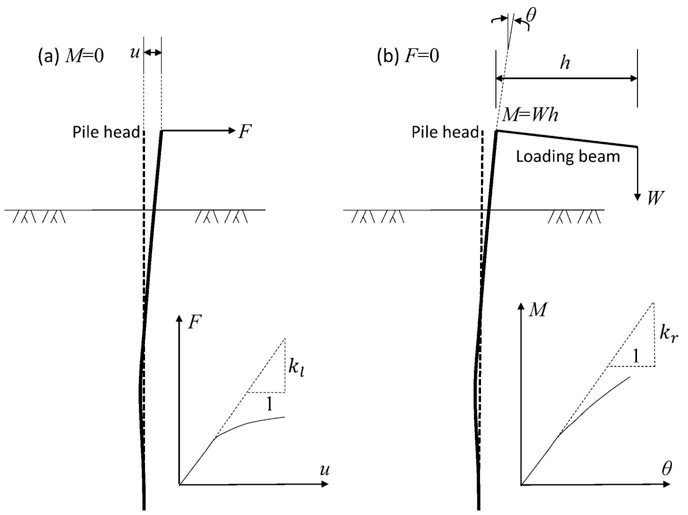

Fig. 3 Static loading test on a monopile: (a) lateral displacement testa and (b) moment test

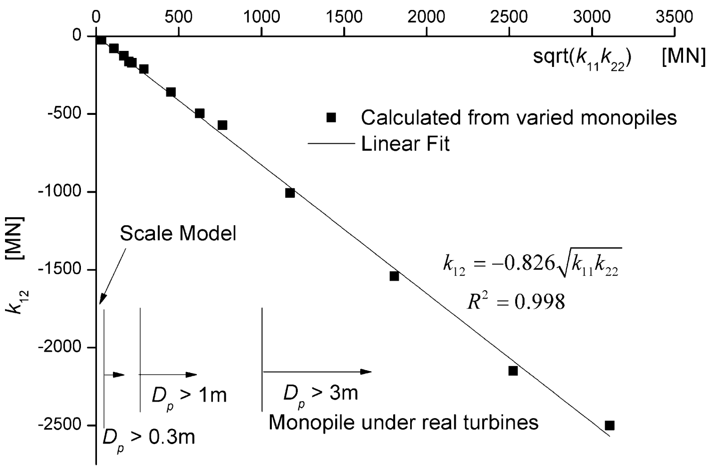

Fig. 4 Relationship between the diagonal and non-diagonal stiffness obtained from *p*-*y* analysis

Substituting Eq. (12) into Eqs. (10) and (11) the elements in the stiffness matrix are calculated by

$$k_{11} = \frac{k_l}{1-\delta^2} \qquad k_{22} = \frac{k_r}{1-\delta^2} \qquad k_{12} = -\frac{\delta}{1-\delta^2}\sqrt{k_l k_r} \tag{13}$$

It appears that the static loading test is the only method to obtain the foundation stiffness through direct measurement. However, for piles in the saturated soils, the difference between the static and dynamic modulus might lead to some errors, which will be discussed in the case studies.

4. Expression of first natural frequency

Based on Rayleigh's method, expression for the natural frequency of a wind turbine-foundation system can be derived. In free vibration, energy is exchanged between the kinetic energy (T) and strain energy (V). Since the maxima of these two types of energy ($T_{\max}$ and $V_{\max}$) are identical, the natural frequency (circular frequency ω) is obtained from

$$\omega^2 = \frac{V_{\max}}{T_{\max}/\omega^2} = \frac{V_{\max}}{\frac{1}{2}\int_0^L m(x)\left[\psi(x)\right]^2 dx + \frac{1}{2}M\left[\psi|_{x=L}\right]^2} \tag{14}$$

where the function ψ denotes the vibration mode. A precise mode shape will lead to the smallest frequency. According to Rayleigh's approach (Clough and Penzien 1993), a hypothetical mode shape is introduced as shown in Fig. 5, which is actually the deflection curve of a beam with a small point load on the end. The beam (Euler-Bernoulli beam) is settled on a flexible foundation which is represented by a stiffness matrix. For the first natural frequency, it will be shown that the results calculated from this vibration mode is in good agreement with the measured frequencies. With reference to Fig. 5

$$\psi(x) = Z_0\left(\frac{3x^2L - x^3}{2L^3}\right) + u + \theta x \tag{15}$$

where Z_0 denotes the lateral deflection of the cantilever beam on a fixed base (with infinite foundation stiffness). It is simply given by

$$Z_0 = \frac{PL^3}{3EI} \tag{16}$$

in which P = the small point load on the end of the beam. The magnitude of P is insignificant because it vanishes in the final expression. Deformation of the foundation can be calculated from Eq. (5) as

$$\begin{aligned} u &= \frac{k_{22} - k_{12}L}{k_{11}k_{22} - k_{12}^{\,2}}P \\ \theta &= \frac{k_{11}L - k_{12}}{k_{11}k_{22} - k_{12}^{\,2}}P \end{aligned} \tag{17}$$

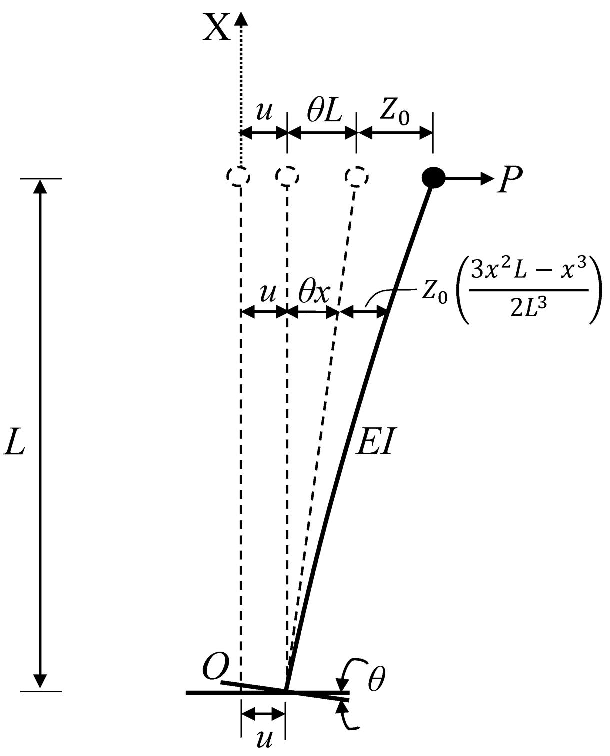

Fig. 5 A beam on flexible foundation with a small point load on the end (the deformation is enlarged to show the relationships)

Strain energy of the system includes the energy of the curved beam and that of the foundation. During the vibration, the strain energy of vertical force (gravity) remains nearly constant, thus it will be ignored in the analysis. With Eqs. (15) and (17), $V_{\max}$ is given by

$$\begin{aligned} V_{\max} &= \frac{1}{2}\int_0^L EI\left[\psi''(x)\right]^2 dx + \frac{1}{2}k_{11}u^2 + \frac{1}{2}k_{22}\theta^2 + k_{12}u\theta \\ &= \frac{1}{2}P^2\left(\frac{L^3}{3EI} + \frac{k_{22} - 2k_{12}L + k_{11}L^2}{k_{11}k_{22} - k_{12}{}^2}\right) \\ &= \frac{1}{2}P\left(Z_0 + u + \theta L\right) \end{aligned} \tag{18}$$

Since the strain energy is equal to the work of load P, $V_{\max}$ can also be given by $V_{\max} = \frac{1}{2}P\psi\big|_{x=L}$, which will lead to the same answer as Eq. (18).

The kinetic energy of the system is expressed as

$$T_{\max} = T_{\max}^B + T_{\max}^M \tag{19}$$

where $T_{\max}^{B}$ is the kinetic energy of the beam, and $T_{\max}^{M}$ denotes the kinetic energy of the top mass. The two parts of kinetic energy are given by

$$\begin{aligned} T_{\max}^{B} &= \frac{\omega^2}{2}\int_0^L m\left[\psi(x)\right]^2 dx = \frac{\omega^2}{2}\int_0^L m\left[Z_0\left(\frac{3x^2L - x^3}{2L^3}\right) + u + \theta x\right]^2 dx \\ &= \frac{\omega^2}{2} mL\left(\frac{33}{140}Z_0{}^2 + u^2 + u\theta L + \frac{1}{3}\theta^2L^2 + \frac{3}{4}Z_0u + \frac{11}{20}Z_0\theta L\right) \\ T_{\max}^{M} &= \frac{\omega^2}{2}M\left[\psi\big|_{x=L}\right]^2 = \frac{\omega^2}{2}M\left(Z_0 + u + \theta L\right)^2 \end{aligned} \tag{20}$$

which can be combined with Eqs. (14) and (18) to provide

$$\omega^2 = \frac{P\left(Z_0 + u + \theta L\right)}{M\left(Z_0 + u + \theta L\right)^2 + mL\left(\frac{33}{140}Z_0{}^2 + u^2 + u\theta L + \frac{1}{3}\theta^2L^2 + \frac{3}{4}Z_0u + \frac{11}{20}Z_0\theta L\right)} \tag{21}$$

With the use of Eqs. (17) and (16) in Eq. (21), load P vanishes and the frequency ω can be expressed by a function of the physical parameters

$$\omega^2 = \frac{\dfrac{L^3}{3EI} + \dfrac{k_{22} - 2k_{12}L + k_{11}L^2}{k_{11}k_{22} - k_{12}{}^2}}{\left\{\begin{array}{l} \left(\dfrac{L^3}{3EI} + \dfrac{k_{22} - 2k_{12}L + k_{11}L^2}{k_{11}k_{22} - k_{12}{}^2}\right)^2 M \\ + \left[\begin{array}{l} \dfrac{33}{140}\left(\dfrac{L^3}{3EI}\right)^2 + \dfrac{L^3}{60EI}\dfrac{11k_{11}L^2 - 26k_{12}L + 15k_{22}}{k_{11}k_{22} - k_{12}{}^2} + \\ \dfrac{\frac{1}{3}k_{11}{}^2L^4 - \frac{5}{3}k_{11}k_{12}L^3 + \frac{7}{3}k_{12}{}^2L^2 + k_{11}k_{22}L^2 - 3k_{22}k_{12}L + k_{22}{}^2}{\left(k_{11}k_{22} - k_{12}{}^2\right)^2} \end{array}\right] mL \end{array}\right\}} \tag{22}$$

To simplify the expression, two dimensionless parameters are defined by

$$\begin{aligned} \varepsilon_u &= \frac{u}{Z_0} = \frac{k_{22} - k_{12}L}{k_{11}k_{22} - k_{12}{}^2}\frac{3EI}{L^3} \\ \varepsilon_\theta &= \frac{\theta L}{Z_0} = \frac{k_{11}L - k_{12}}{k_{11}k_{22} - k_{12}{}^2}\frac{3EI}{L^2} \end{aligned} \tag{23}$$

where ε_u = coefficient of lateral displacement; ε_θ = coefficient of rotational displacement. For a given wind turbine-foundation system, both ε_u and ε_θ are just dimensionless constants. With the use of Eq. (23), Eq. (21) can now be written as

$$\omega = \sqrt{\frac{\left(1 + \varepsilon_u + \varepsilon_\theta\right)\frac{3EI}{L^3}}{\left(1 + \varepsilon_u + \varepsilon_\theta\right)^2 M + \left(\frac{33}{140} + \varepsilon_u{}^2 + \frac{1}{3}\varepsilon_\theta{}^2 + \frac{3}{4}\varepsilon_u + \frac{11}{20}\varepsilon_\theta + \varepsilon_u\varepsilon_\theta\right)mL}} \tag{24}$$

which is a simple expression that can even be worked out with a pocket calculator. It can also be used to provide a sensitivity analysis.

For a beam fixed at the bottom, it is obvious that $\varepsilon_u = \varepsilon_\theta = 0$, thus Eq. (24) reduces to

$$\omega = \sqrt{\frac{3EI}{\left(M + \frac{33}{140}mL\right)L^3}} \tag{25}$$

Eq. (25) is exactly the same equation as Eq. (1). Thus Eq. (24) is actually the generalization of the classical case so that a non-diagonal stiffness matrix is considered in the dynamic model.

Here it can be argued that if Eq. (6) is used (a diagonal stiffness matrix), Eq. (22) becomes

$$\omega = \sqrt{\frac{\frac{L^3}{3EI} + \frac{k_r + k_l L^2}{k_l k_r}}{\left\{\begin{array}{l}\left(\frac{L^3}{3EI} + \frac{k_r + k_l L^2}{k_l k_r}\right)^2 M \\ + \left[\frac{33}{140}\left(\frac{L^3}{3EI}\right)^2 + \frac{L^3}{60EI}\frac{11k_l L^2 + 15k_r}{k_l k_r} + \frac{\frac{1}{3}k_l^{\,2} L^4 + k_l k_r L^2 + k_r^{\,2}}{\left(k_l k_r\right)^2}\right] mL\end{array}\right\}}} \tag{26}$$

which is the expression of the first natural frequency for the model of uncoupled springs. Eq. (26) is simpler than Eq. (22). But compared to Eq. (24), Eq. (26) provides very less advantage in calculations.

If the damping ratio, ζ, is considered in the analysis, a coefficient of $\sqrt{1-\zeta^2}$ should be multiplied in the right-hand-side of Eq. (24).According to Arany *et al.* (2016), the total damping is typically between 2% and 8% for an operational turbine. Therefore, the coefficient of $\sqrt{1-\zeta^2}$ is very close to unity (0.997~1) and thus can be ignored in the calculations of the first natural frequency.

5. Validation of the proposed equation for monopiles and discussion

In this section, the results of proposed expressions are validated against the experimental measurements for real turbines and model tests. The analyzed real and model turbines are presented in Table 1, as well as references to the sources of data. For the two real turbines, Lely A2 and A3 in Netherlands, the input parameters in the *p*-*y* analysis are available in Zaaijer (2002a). Foundation stiffness of Model A is also obtained from *p*-*y* method. The calculations shown in Section 3.1 are carried out for the two real turbines and Model A.

For Models B-D, the spring stiffness (k_l and k_r) were measured directly from static loading tests (Bhattacharya and Adhikari 2011). Thus the elements in the stiffness matrix can be obtained as shown in Section 3.2. The spring stiffness and natural frequency were measured after 14,400 cycles of 3P loading so that the characteristic of model turbine and foundation has held relatively steady. Table 2 shows the obtained stiffness for all cases.

The natural frequencies calculated from different expressions are shown in Table 3. Varied analytical expressions and an empirical method are carried out for all the cases. The analytical expressions are based on the three mathematical models as shown in Fig. 1. For the fixed base model, uncoupled springs and stiffness matrix, Eqs. (1), (26) and (24) are used respectively.

5.1 Discussion on analytical results of stiffness matrix

The measured natural frequencies for each case are available in the literature (Bhattacharya and Adhikari 2011, Yu *et al*. 2014, Zaaijer 2006). Comparison between the results of varied expressions and the measured values are also shown in Table 3. The proposed expression based on stiffness matrix gives reasonable predictions for both the real turbines and the scale models. In the first four cases (two real turbines, Models A and B), the errors are quite small (±1.2%). Larger errors are observed in Models C (10.6%) and D (-16.2%). Since the foundation stiffness was obtained from static loading tests for these two models, the errors might be attributed to the difference between the static and dynamic modulus of saturated soils.

In the case of Model C, the model pile was inserted into the saturated sand. The foundation stiffness might be reduced because of some sort of shock liquefaction, thus the calculation based on static modulus tends to overestimate the natural frequency. The turbines Lely A2 and A3 are also founded mainly on saturated sands. But the stiffness matrix is obtained from *p*-*y* curves for these two turbines. According to API (2007), the cyclic *p*-*y* springs are significantly softer than the static ones for sandy soils. Therefore, the reduction in dynamic stiffness is taken into account for the two real turbines and the predicted natural frequencies are quite close to the measured values.

In the case of Model D, the model pile was embedded in saturated clay. For this model turbine, the natural frequency is underestimated by the analytical solution based on stiffness matrix. During the vibration, it appears that the pore water in saturated clay is unable to move. With such a restriction, the clay is actually stiffer than that in the static loading condition, because a consolidation process is allowed for the latter one. This might explain why the natural frequency is underestimated for model D. For the two real turbines, Lely A2 and A3, the *p*-*y* method also ignores the difference between the dynamic and static modulus of clays. But the clay layer is quite thin for these two turbines, thus the foundation stiffness is basically dominated by the sand layer and the deviation is not revealed.

5.2 Comparison between results of different expressions

The results of formulas available in the literature, i.e. an empirical formula based on stiffness matrix (Arany *et al*. 2016) and an analytical expression based on uncoupled springs (Adhikari and Bhattacharya 2011), are also shown in Table 3. It appears that the performance of the empirical formula is not so stable. For the first three cases (two real turbines and Model A), the empirical formula gives very accurate predictions on natural frequency. But large deviations (up to 78%) are observed in the other cases. From a physical point of view, entanglement between the parameters of mass and stiffness is shown in Eq. (24). Such entanglement is also shown in the analytical expressions based on the uncoupled springs (Adhikari and Bhattacharya 2011). This means that the empirical factors (C_R and C_L) might not be determined by the stiffness parameters alone. In another word, the mass parameters should play a role in Eq. (8). Thus the empirical formula somehow fails for the last three model turbines.

Table 1 Properties of upper structure, monopile and soil for real wind turbines and model tests

	Turbine (or model test) ID	Lely(A2)	Lely(A3)	Model A	Model B	Model C	Model D
	Reference	Zaaijer (2002a)		Yu *et al.* (2014, 2015)	Bhattacharya and Adhikari (2011)		
Tower	Top Mass M (kg)	32000		1.0	1.348		
	Height L (m)	39.0		1.0	1.0		
	Diameter D_T (m)	1.9-3.2 (conical)		0.043 (uniform)	0.038 (uniform)		
	Wall thickness t_T (m)	0.012		0.002	0.0016		
	EI (Nm^2)	22×10^9*		11394	2125		
	m (kg/m)	751.11		2.0	0.576		
Monopile	Full length (m)	26	28	0.45	0.5		
	Embedded length (m)	13.9	20.9	0.45	0.5		
	Diameter D_P (m)	3.2	3.7	0.043	0.022		
	Wall thickness t_P (m)	0.035	0.035	0.002	0.0013		
	Material	Steel	Steel	Steel	Dural alloy	Dural alloy	Dural alloy
	Young's modulus (GPa)	210	210	210	70	70	70
Soil conditions	Upper layer	Soft clay 2m thick s_u=20kPa**, γ'=8kN/m^3**	4m thick	Dry sand uniform φ'=36°***, γ_d=16.8kN/m^3***	Dry sand uniform	Saturated sand uniform	Saturated clay uniform
	Sublayer	Dense sand φ'=38°**, γ'=11kN/m^3**					

* Equivalent *EI* considering the effect of tapering (Adhikari and Bhattacharya 2012).
** Typical value for the soil type.
***Measured and reported in the literature.

Indicated in Table 3 are also the comparisons between the results of different mathematical models. It is obvious that the fixed base model gives the highest prediction of natural frequency, while the model of stiffness matrix gives the smallest one. The results calculated from the uncoupled springs are 2~40% higher than those calculated from the stiffness matrix. Thus the effects of coupled stiffness (k_{12}) are not negligible. This means that the expression based on stiffness matrix is more appropriate than that based on uncoupled springs. Similar opinion can be found in Arany *et al.* (2015). Among all the formulas, it is shown that the proposed analytical solution based on stiffness matrix gives the most reasonable predictions.

Table 2 Parameters of the stiffness matrix and uncoupled springs for the real wind turbines and models

Turbine (or model test) ID		Lely(A2)	Lely(A3)	Model A	Model B	Model C	Model D
Methods		*p*-*y* curves	*p*-*y* curves	*p*-*y* curves	Static loading test*		
Elements in stiffness matrix	k_{11} (MN/m)	94	242	1.48	0.118	0.112	0.0110
	k_{12} (MN)	-1040	-2230	-0.300	-0.0170	-0.0156	-0.00318
	k_{22} (MN·m)	15800	28400	0.0866	0.00359	0.00318	0.00135
Spring stiffness	k_l (MN/m)	24.5	66.5	0.441	0.0375	0.0357	0.0035
	k_r (MN·m)	4130	7810	0.0257	0.00114	0.00101	0.000428

* For models B-D, the spring stiffness were measured directly by Bhattacharya and Adhikari (2011), the elements in stiffness matrix are calculated from Eq. (13) with δ=0.826

Table 3 Measured and predicted natural frequencies of the real wind turbines and models

Turbine (or model test) ID		Lely(A2)	Lely(A3)	Model A	Model B	Model C	Model D
Analytical expression (Hz)	1 Fixed base	0.851		24.3	10.4	10.4	10.4
	2 Uncoupled springs*	0.696	0.761	15.0	3.94	3.75	2.42
	3 Uncoupled springs**	0.740	–	–	3.62	3.43	2.76
	4 Stiffness matrix*	0.641	0.728	13.3	3.52	3.35	1.97
5 Empirical formula*** (Hz)		0.643	0.712	13.3	2.28	2.07	0.508
6 Measured frequency (Hz)		0.634	0.735	13.3	3.52	3.03	2.35
Difference between 3 and 6 (%)**		16.8	–	–	2.84	13.2	17.4
Difference between 4 and 6 (%)*		1.14	-0.98	-0.15	0.00	10.6	-16.2
Difference between 5 and 6 (%)***		1.42	-3.13	-0.15	-35.2	-31.7	-78.4
Difference between 2 and 4 (%)		8.62	4.58	13.1	11.9	11.9	22.8
Difference between 3 and 4 (%)		15.47	–	–	2.84	2.39	40.10

* Present study: Uncoupled springs by Eq. (26); Stiffness matrix by Eq. (24)
** Results of the analytical solution based on uncoupled springs proposed by Adhikari and Bhattacharya (2011).
*** Results of the empirical formula based on stiffness matrix proposed by Arany *et al.* (2016) , i.e., Eq. (7)

6. Conclusions

A new analytical solution is derived for the natural frequency of wind turbine towers supported by monopile. The tower is modelled as a Euler-Bernoulli beam with a top mass and the foundation is represented by a stiffness matrix. The obtained expression is based on pure physical parameters and thus can be used for a quick assessment of the natural frequencies of both the real turbines and the small-scale models. A relationship is introduced between the diagonal and non-diagonal element, so that the stiffness matrix can be obtained from either the *p-y* analysis or the direct measurements of static loading test. Validation against the measured frequencies shows that the proposed expression gives reasonable predictions for both the real and the model turbines. For two of the model turbines, some errors (up to 16%) were observed which might be attributed to the difference between the dynamic and static modulus of saturated soils. It is shown that the proposed expression is quite simple to use, and it is more reasonable than the analytical and the empirical formulas available in the literature.

Acknowledgements

The research presented here was supported by the National Natural Science Foundation of China (No. 41672264), the Zhejiang Provincial Natural Science Foundation of China (No. LQ18E080001), and by the Natural Science Foundation of Ningbo City (No. 2017A610304). Grateful appreciation is expressed for this support.

References

Adhikari, S. and Bhattacharya, S. (2011), "Vibrations of wind-turbines considering soil-structure interaction". *Wind Struct*., **14**(2), 85-112.
Adhikari, S. and Bhattacharya, S. (2012), "Dynamic analysis of wind turbine towers on flexible foundations", *J. Shock Vib*., **19**(1), 37-56.
American Petroleum Institute (API) (2007), *Recommended Practice for Planning, Designing and Constructing Fixed Offshore Platforms-Working Stress Design*.
Arany, L., Bhattacharya, S., Adhikari, S., Hogan, S.J. and Macdonald, J.H.G. (2015), "An analytical model to predict the natural frequency of offshore wind turbines on three-spring flexible foundations using two different beam models", *Soil Dyn. Earthq. Eng.*, **74**, 40-45.
Arany, L., Bhattacharya, S., Macdonald, J.H.G. and Hogan, S.J. (2016), "Closed form solution of Eigen frequency of monopile supported offshore wind turbines in deeper waters incorporating stiffness of substructure and SSI", *Soil Dyn. Earthq. Eng*., **83**, 18-32.
Bhattacharya, S. (2014), "Challenges in design of foundations for offshore wind turbines", *Eng. Technol. Ref.*, 1-9.
Bhattacharya, S. and Adhikari, S. (2011), "Experimental validation of soil-structure interaction of offshore wind turbines", *Soil Dyn. Earthq. Eng*., **31**, 805-816.
Bhattacharya, S., Lombardi, D. and Muir Wood, D. (2011), "Similitude relationships for physical modelling of monopile-supported offshore wind turbines", *Int. J. Phys. Model. Geotech.*, **11**(2), 58-68.
Bhattacharya, S., Nikitas, N., Garnsey, J., Alexander, N.A., Cox, J., Lombardi, D., Muir Wood, D. and Nash, D.F.T. (2013a), "Observed dynamic soil-structure interaction in scale testing of offshore wind turbine foundations", *Soil Dyn. Earthq. Eng.*, **54**, 47-60.
Bhattacharya, S., Cox, J.A., Lombardi, D. and Wood Muir Wood, D.M. (2013b), "Dynamics of offshore

wind turbines supported on two foundations", *Proc. ICE - Geotech. Eng.*, **166**, 159-169.
Blevins, R.D. (2001), *Formulas for Natural Frequency and Mode Shape* (Malabar, FL, USA: Krieger Publishing Company).
Clough, R.W. and Penzien, J. (1993), *Dynamics of Structures* (New York: Mcgraw-Hill).
DNV (2014), *DNV-OS-J101 Design of Offshore Wind Turbine Structures* (Høvik,Norway).
Jafri, S.M., Eltaher, A. and Jukes, P. (2011), "Dynamics of offshore wind turbines". *Proc. Int. Offshore Polar Eng. Conf.*, **8**, 277–283.
Lombardi, D., Bhattacharya, S. and Muir Wood, D. (2013), "Dynamic soil-structure interaction of monopile supported wind turbines in cohesive soil", *Soil Dyn. Earthq. Eng.*, **49**, 165-180.
van der Tempel, J. and Molenaar, D.P. (2003). "Wind turbine structural dynamics-a review of the principles for modern power generation, onshore and offshore", *Wind Eng.*, **26**, 211-222.
Yu, L., Bhattacharya, S., Li, L. and Guo, Z. (2014), "Dynamic characteristics of offshore wind turbines on different types of foundations", *Ejge*, **19**, 2917-2936.
Yu, L.Q., Wang, L.Z., Guo, Z., Bhattacharya, S., Nikitas, G., Li, L.L. and Xing, Y.L. (2015), "Long-term dynamic behavior of monopile supported offshore wind turbines in sand", *Theor. Appl. Mech. Lett.*, **5**(2), 80-84.
Zaaijer, M.B. (2002a), "Sensitivity analysis for foundations of offshore wind turbines", OWTES Task 4.1.
Zaaijer, M.B. (2002b), "Foundation models for the dynamic response of offshore wind turbines", *Mar. Renew. Energy Conf.*
Zaaijer, M.B. (2006), "Foundation modeling to assess dynamic behaviour of offshore wind turbines", *Appl. Ocean Res.*, **28**(1), 45-57.

CC